Synthesis of 2-Methyl-3-indolylacetic Derivatives as Anti-Inflammatory Agents That Inhibit Preferentially Cyclooxygenase 1 without Gastric Damage

Elisa Perissutti,[†] Ferdinando Fiorino,[†] Christian Renner,[‡] Beatrice Severino,[†] Fiorentina Roviezzo,[§] Lidia Sautebin,[§] Antonietta Rossi,[§] Giuseppe Cirino,[§] Vincenzo Santagada,[†] and Giuseppe Caliendo*[,†]

Dipartimento di Chimica Farmaceutica e Tossicologica and Dipartimento di Farmacologia Sperimentale, Università di Napoli "Federico II", Via D. Montesano, 49, 80131 Napoli, Italy, and Max-Planck-Institute of Biochemistry, Am Klopferspitz 18, 82152 Martinsried, Munich, Germany

Received July 12, 2006

Novel substituted 2-methyl-3-indolylacetic derivatives were synthesized and evaluated for their activity in vitro and in vivo on COX-1 and COX-2. Active compounds were screened to determine their gastrointestinal tolerability in vivo in the rat. Results showed that **3** and **4** preferentially inhibited COX-1 in vitro and in vivo. MD simulations indicated an induced fit for COX-1 but not for COX-2, probably because of a lower plasticity of the latter.

Introduction

Nonsteroidal anti-inflammatory drugs (NSAIDs) are potent cyclooxygenase (COX) inhibitors that are widely used for the treatment of autoimmune and chronic inflammatory diseases.[1] COX performs the first step in the conversion of arachidonic acid into inflammatory prostaglandins. It adds two oxygen molecules to arachidonic acid, initiating a set of reactions that will ultimately create a host of unusual molecules. Two distinct isoforms have been identified separately: COX-1 and COX-2. COX-1 is known as a housekeeping enzyme constitutively expressed in most mammalian tissues and is responsible for keeping the stomach lining intact and maintaining functional kidneys. While COX-2 is constitutively expressed only in kidney, brain, and ovaries, it can be rapidly expressed during inflammatory conditions by proinflammatory stimuli such as IL-1, TNF-α, and LPS and agents such as carrageenan, releasing metabolites that are used to induce inflammation, fever, and pain.[2]

NSAIDs can block the binding of arachidonic acid in the COX active site; it is thought to result from initial binding to the Arg^{120} and acetylation of the Ser^{530} hydroxyl group (in the case of aspirin) in the primary COX binding site. After this interaction the enzyme is blocked and the inflammatory reaction and the associated pain perception are controlled. However, the chronic usage of these drugs is associated with the induction of gastrointestinal mucosal lesions, perforations, and bleeding in part of the population. Decreased renal functions have been observed in some patients. The reason is that these COX inhibitors also inhibit COX-1 to produce the necessary prostaglandins.[3] Selective COX-2 inhibitors such as celecoxib elicit effective anti-inflammatory activity devoid of the ulcerogenic effects associated with the use of NSAIDs such as aspirin, which inhibit COX-1 and COX-2.[4,5] However, the lack of effect on COX-1 does not allow COX-2 inhibitors to exert an antiplatelet effect. Recently COX-2 inhibitors have been shown to produce cardiovascular side effects and some of them such as rofecoxib have been retired from the market.[6]

* To whom correspondence should be addressed. Phone: 0039-081-678649. Fax: 0039-081-678649. E-mail: caliendo@unina.it.

[†] Dipartimento di Chimica Farmaceutica e Tossicologica, Università di Napoli "Federico II".

[‡] Max-Planck-Institute of Biochemistry.

[§] Dipartimento di Farmacologia Sperimentale, Università di Napoli "Federico II".

We have designed and synthesized novel substituted 2-methyl-3-indolylacetic derivatives in an attempt to obtain COX-1 inhibitors sparing the gastrointestinal (GI) side effects. These new derivatives present an acidic function related to a basic moiety. In particular, the synthesized structures possess in position 1 a *N*-methyl-4-piperidinyl ring as a basic and nonaromatic pharmacophoric portion present in some drugs that have shown COX-2 selectivity (i.e., Nimesulide,[7] NS-398,[8] RWJ-63356[9]), with the purpose of verifying if these structural changes would shift selectivity toward COX-2. All synthesized compounds were screened in vitro for COX-1 and COX-2 inhibitory effects and then tested in vivo in carrageenin-induced mouse paw edema. Compounds showing a favorable profile were screened for GI tolerability in vivo in the rat and in specific pain assays. Molecular modeling simulations were performed to rationalize the inhibitory activity and to analyze the relevant interactions between enzyme and ligand.

Chemistry

The synthetic route for the preparation of substituted 2-methyl-3-indolylacetic derivatives (**3**−**6**) is reported in Scheme 1. The aniline derivative **1** was obtained by a reductive amination of *p*-anisidine with 1-methylpiperidin-4-one in presence of sodium cyanoborohydride[10] and molecular sieves,[11] which serve simultaneously as a dehydrating agent and as a catalyst. The nitrosation followed by a reduction step with $LiAlH_4$ afforded the hydrazine **2** in 90% yield. The Fischer indole reaction of hydrazine **2** was performed as a "one-pot" reaction under acidic conditions yielding **3** (yield 71%) (Scheme 1). Starting from **3**, we obtained **4** by ethyl ester saponification and **6** by reaction with HI and acetic anhydride at room temperature. Compound **5** was obtained by treating **4** with HI and acetic anhydride at 130 °C (Scheme 2). Analytical purification of each product (Table 1) was obtained by chromatography on silica gel column and by crystallization from the appropriate solvent. All new compounds gave satisfactory elemental analysis results (C, H, N) and were characterized by ^1H NMR spectroscopy.

Results and Discussion

All the synthesized compounds were screened for COX selectivity in an in vitro cell based assay. Stimulation of J774 macrophages with arachidonic acid (15 μM) for 30 min induced a significant increase ($p < 0.001$) of PGE_2 (3.6 ± 0.3 ng × $l0^6$

10.1021/jm0608199 CCC: $33.50
Published on Web 12/21/2006

Scheme 1

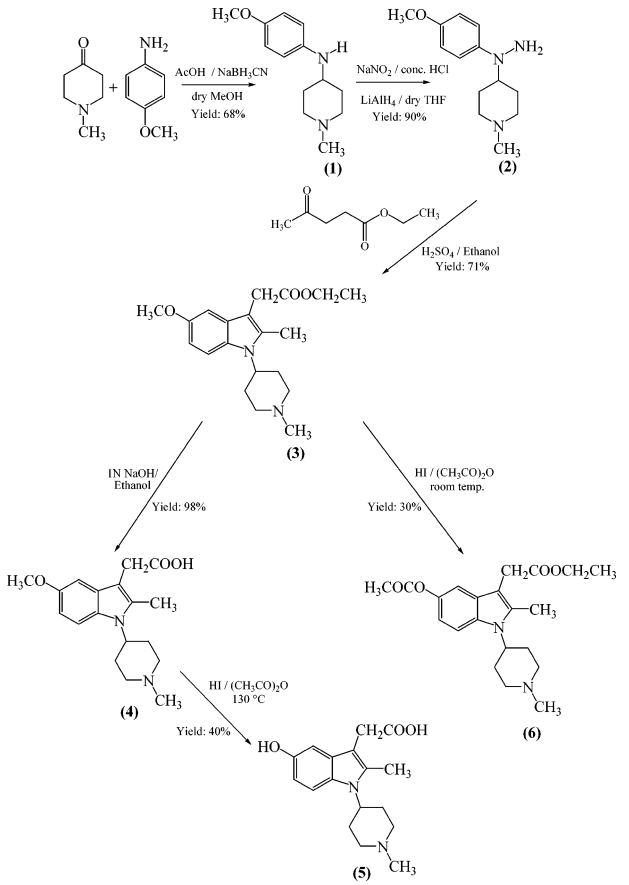

cells) levels in comparison to unstimulated cells (<0.0125 ng $\times$ l0^6 cells). In the presence of increasing concentrations (0.01−100 μM) of indomethacin (a nonselective COX-1/COX-2 inhibitor) a concentration-dependent inhibition of PGE_2 biosynthesis was observed (Figure 1A). **3** and **4** (0.01−100 μM) derivatives, related to indomethacin, exerted a similar concentration-dependent inhibition on PGE_2 generation, although they were less potent than indomethacin (Figure 1A). At the highest concentration (100 μM), PGE_2 production was significantly inhibited by indomethacin (88%, $p < 0.001$), **4** (64%, $p < 0.001$), and **3** (58%, $p < 0.001$), with **4** and **3** displaying equivalent inhibitory activity on COX-1. At lower concentration (10 μM), indomethacin still significantly ($p < 0.001$) inhibited PGE_2 production to about 75%, displaying a more powerful inhibition than **4** (57%, $p < 0.001$) and **3** (37%, $p < 0.001$). **5** and **6** were inactive at all the tested concentrations (0.01−100

Table 1.

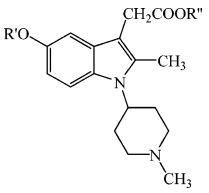

compd	R′	R″	formula[a]	mp, °C	cryst solvent[b]	yield, %
3	CH_3	CH_2CH_3	$C_{20}H_{28}N_2O_3$	68−70	a	71
4	CH_3	H	$C_{18}H_{24}N_2O_3$	172−173	a	98
5	H	H	$C_{17}H_{22}N_2O_3$	204−206	a + b	40
6	$COCH_3$	CH_2CH_3	$C_{21}H_{28}N_2O_4$	98−99	a	30

[a] Satisfactory microanalyses obtained: C, H, N values are within ±0.4% of theoretical values. [b] Crystallization solvents: (a) diethyl ether; (b) ethyl alcohol.

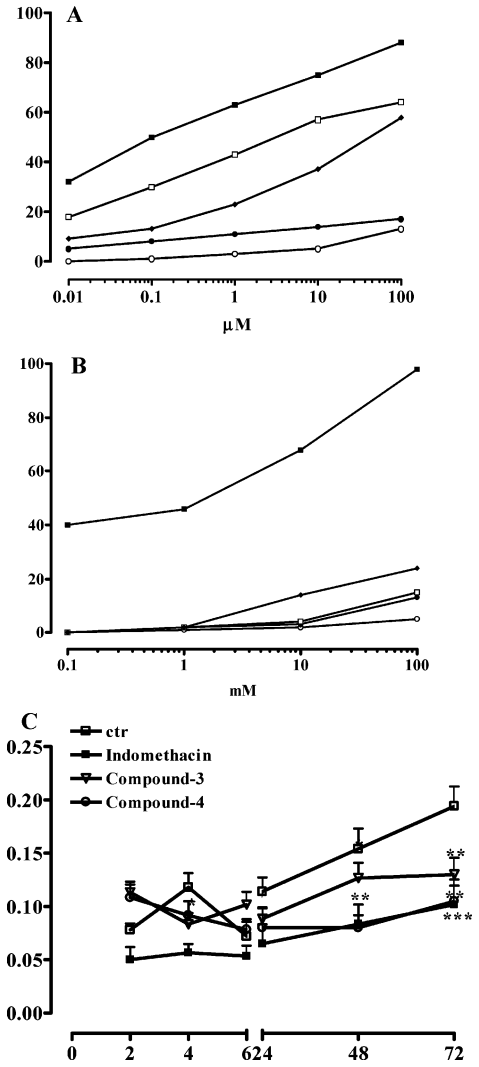

Figure 1. (A) Effect of derivatives **3**−**6** vs indomethacin on COX-1 activity. **3** and **4** display a good inhibitory activity on COX-1, while **5** and **6** are weak inhibitors. (B) Effect of derivatives **3**−**6** vs DFU, a selective COX-2 inhibitor, on COX-2 activity. (C) Effect of derivatives **3** and **4** vs indomethacin on mouse paw edema.

μM). Conversely, a significant ($p <$ 0.00l) concentration-dependent inhibition of PGE_2 production (Figure 1B) was induced by 5,5-dimethyl-3-(3-fluorophenyl)-4-(4-methylsulphonyl)phenyl-2(5*H*)-furanone (DFU), a selective COX-2 inhibitor (0.1−100 μM) while the new synthesized derivatives were ineffective with the only exception of **3**, which exerted 24% of inhibition ($p < 0.05$) at the highest tested concentration (Figure 1B). Stimulation with LPS followed by wash-out and 30 min of incubation with arachidonic acid (15 pM) induced a significant ($p < 0.001$) increase of PGE_2 generation (31.6 ± 2. ng $\times$ 10^6 cells) in comparison to unstimulated cells (0.62 ± 0.072 ng $\times$ l0^6 cells). After this preliminary screening, **3** and **4** were selected for the subsequent in vivo screening. They were screened for their anti-inflammatory activity in the mouse edema assay, while the analgesic activity was assessed by using two different assays, e.g., formalin paw licking and acetic acid induced writhing. **3** and **4** displayed significant anti-inflammatory activity in carrageenin-induced mouse paw edema; **3** was especially equipotent with indomethacin (Figure 1C). **3** and **4** displayed an analgesic activity comparable to indomethacin in the second phase of formalin paw licking (Figure 2A), while they were ineffective in the first phase (data not shown). In the writhing assay, **3** and **4** displayed a dose related effect with **4**

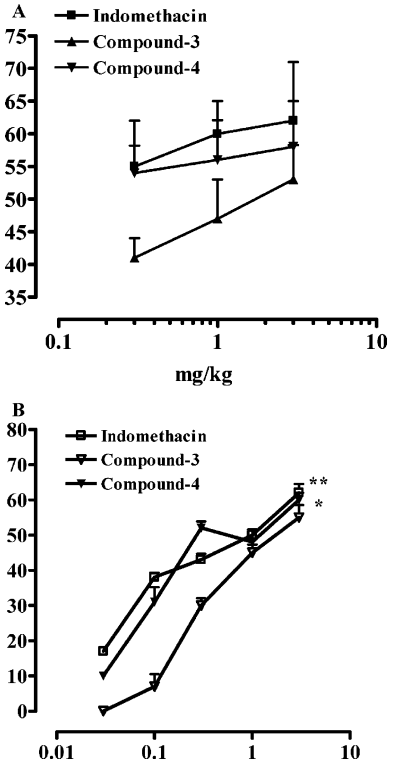

Figure 2. (A) Analgesic effect of indomethacin, **3**, and **4** on the second phase of paw licking assay. Data are expressed as percent of inhibition. Control value was 25 ± 4 s. (B) Analgesic effect of indomethacin, **3**, and **4** on acetic acid induced writhing. Data are expressed as percent of inhibition. Control value was 39.8 ± 5.3.

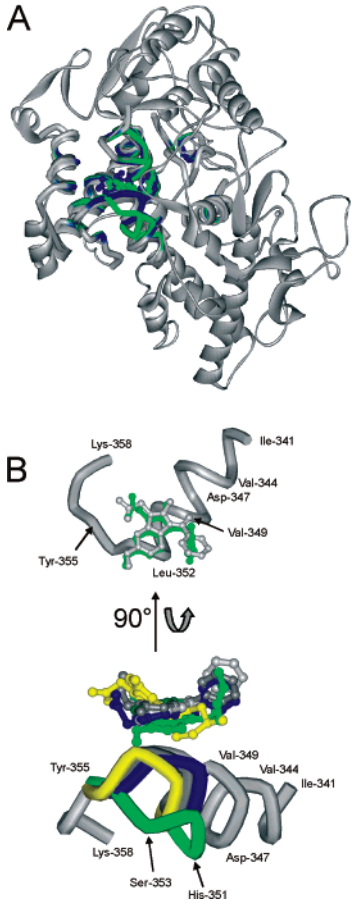

Figure 3. (A) Crystal structure 4COX of COX-2 in complex with indomethacin in light-gray with the flexible binding site of the COX-1/indomethacin and COX-1/**4** complex models in blue and green, respectively. (B) Ligand and the conformation of the loop Val-349 to Tyr-355 at the end of the 300 K simulation for the COX-2/indomethacin (dark-gray), COX-1/indomethacin (blue), COX-2/**4** (yellow), and COX-1/**4** (green) complexes. The X-ray structure 4COX is again shown in light-gray as reference.

showing the better profile (Figure 2B). Interestingly, we have also found that the ester derivative **3** is completely hydrolyzed after 30 min to the corresponding acid derivative **4** by liver metabolism. This evidence was verified by specific assays performed on liver or mice plasma using HPLC analysis. Importantly, **3** and **4** were devoid of GI damaging activity in the rat GI damage assay. In the GI damage assay, indomethacin caused a gastric damage of 50 ± 8 mm and **3** of 0.6 ± 0.03 mm, while **4** did not cause any damage in any of the six treated rats. These data imply that the structural modification operated on **4** preserved the anti-inflammatory and analgesic features of indomethacin but markedly reduced the GI side effects. The finding that a selective COX-1 inhibitor with anti-inflammatory activity (**1** and **2**) does not display GI side effects could be contrary to present knowledge. However, it has been shown that SC560, a selective COX-1 inhibitor, does not cause GI damage even though it inhibits PG synthesis in rat stomach and platelet COX-1 activity.[12] More recently SC560 has been confirmed to have anti-inflammatory activity independent of COX-1 inhibition[13] and to be analgesic in rats.[14]

Molecular Modeling. Available crystal structures of COX-1 and COX-2 in complex with ligands are a solid experimental basis for computer modeling calculations of the new **3**−**6** in complex with COX-1 or COX-2. Unbiased starting models were generated on the basis of the X-ray structure of the COX-2/indomethacin complex[15] (PDB code 4COX; for details see the Experimental Section). During the molecular dynamics (MD) simulation the ligand and a 7 Å binding site on the protein were allowed to move freely with the flexible binding site comprising all amino acid residues of the COX enzyme that had in the 4COX structure at least one atom closer than 7 Å to any atom of indomethacin (see Figure 3A). The parts of the protein far from the ligand binding site were fixed to avoid disintegration of the global fold at higher temperatures. Steric clashes and unfavorable interactions of the initial model were relaxed during minimization and simulation at low temperature (100 K) for 50 ps. The subsequent productive period of 100 ps at 300 K was followed by 50 ps at 500 K to test for stability of the resulting complexes. Generally, rearrangements were observed upon heating to 300 K, but the resulting structures remained fairly stable at 300 K. Further heating to 500 K led to increased fluctuations, but ligands never left the binding site and the binding mode was conserved throughout. Note that conformational sampling at 50 ps at 500 K is quite effective and corresponds to some microseconds at 300 K. Figure 3B shows that **4** induces rearrangements within the protein environment that are significantly more pronounced for COX-1 compared to COX-2. This differential effect is exerted by **3**−**6** ligands but only to minor extents by indomethacin, in agreement with the low specificity of indomethacin with respect to the two COX isoforms. The presence of the charged basic piperidine ring of **3**−**6** in place of the phenyl ring of indomethacin, which occupies the hydrophobic pocket in the 4COX X-ray structure (see Figure 4A), leads to a displacement of the **3**−**6** ligands that in turn appear to induce conformational changes to the protein. For COX-2 these changes are small and the loss of binding to the hydrophobic pocket renders **3**−**6** as ineffective inhibitors of COX-2 (Figure 1B). Conversely, in simulations of the COX-1 complexes a new extended hydrophobic patch is formed because

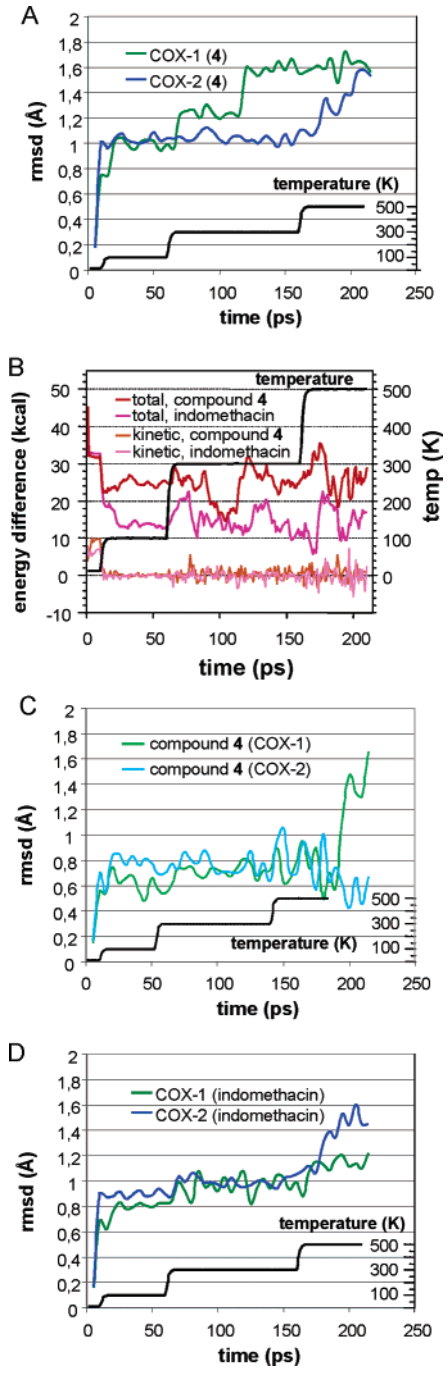

Figure 4. Energies and rmsd values of COX complexes in modeling calculations. The rmsd values are calculated for heavy atoms. In the case of the enzyme only, they were calculated for heavy atoms of the flexible binding site. The temperature curve in black is always shown for reference with a scale given on the right side of the graph. (A) The rmsd values indicating structural rearrangements for both isoforms of the COX/**4** complex. (B) Energies of the complexes with **4** and indomethacin reported as the energy difference of the COX-2 complex minus the COX-1 complex . The kinetic energy difference (corrected for the slightly different numbers of moving atoms) is fluctuating around zero, as expected. C) flexibility of 4 in both COX complexes. (D) The rmsd values of COX-1 and COX-2 complexes with the unselective indomethacin (cf. panel A).

of structural changes brought about by the **3**−**6** ligands, most prominently in loop 351−355 (Figure 3). In that case the ligands can recover their inhibitory activity by hydrophobic interactions between this patch and the indole moiety (Figure 4B). The differences among the **3**−**6** activities correlate with the 5-substituent (OH, OMe, OAc) and are likely due to the differential hydrophobicity and size of the three substituents. A remarkable feature is that the specificity thus arises not from structural differences of COX-1 and COX-2 (the binding sites are basically identical with very few differences in sequence) but from different plasticities of the protein structures, at least around the binding site (Figure 5). Higher *B* factors for COX-1 (PDB code 1DIY, average *B* factor of 45.0 ± 12.4) than for COX-2 (PDB code 1CVU, average *B* factor of 27.6 ± 8.3), both crystallized with the identical ligand arachidonic acid, support the idea of higher flexibility in the former protein. The generally accepted concept of the "induced fit" is thus transformed into a "selectively induced fit" for **3**−**6**. It is speculated that the structural changes are related to the fact that less severe side effects are observed for **3**−**6**. In agreement with this hypothesis is the observation that indomethacin in the MD simulations does not induce pronounced changes to the COX-2 structure.

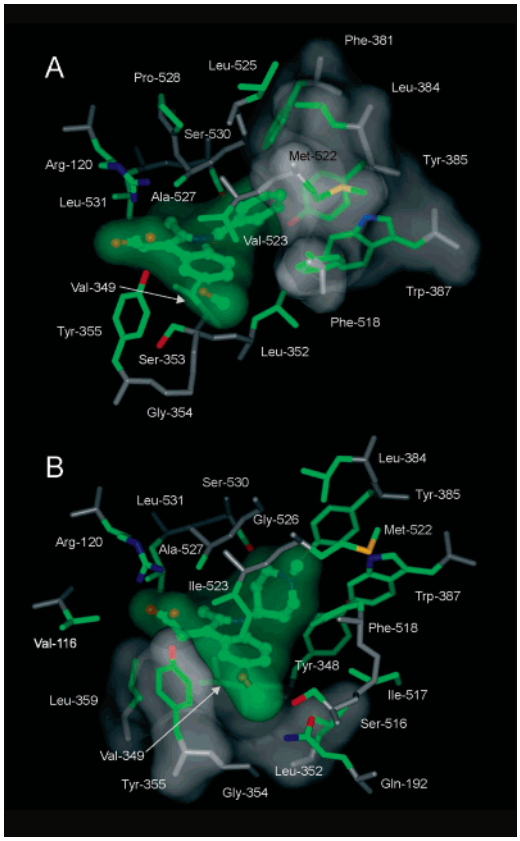

Figure 5. Binding site of the COX enzyme. Protein side chains and the ligand, highlighted by a transparent green surface, are in atom colors, and the protein backbone is in gray. (A) Binding of indomethacin to COX-2 in the 4COX crystal structure. The hydrophobic pocket is indicated by the transparent white surface. (B) Binding of **4** to COX-1 in the calculated model. The newly formed hydrophobic path is indicated by the transparent white surface.

Conclusions

MD simulations show that the **3**−**6** inhibitors, because of the presence of the polar piperidine, cannot bind to the hydrophobic pocket in the COX binding site. However, COX-1 structural rearrangements induced by the ligands seem to form a new hydrophobic interaction site close to the indole moiety that allows recovery of inhibitory activity, at least for suitably 5-substituted compounds. The lower plasticity of COX-2 does not allow these conformational changes to occur and thus prevents activity. Selectivity is thus achieved by a selective

propensity of the protein to the induced fit. In this respect, our data have shed new light on the chemical requisites for designing new COX inhibitors. **3** and **4** derivatives, which present an acidic function related to a basic moiety, preferentially inhibit COX-1 in vitro and are analagesic and anti-inflammatory in vivo. In addition and most importantly, both compounds appear to be devoid of gastric effects.

Experimental Section

Chemistry. All reagents were commercial products purchased from Aldrich. Melting points were determined using a Kofler hot-stage apparatus and are uncorrected. ^{1}H NMR spectra were recorded on a Bruker AMX-500 instrument. All spectra were recorded in $CDCl_3$ or CD_3OD. Chemical shifts are reported in ppm using Me_4-Si as the internal standard. The following abbreviations are used to describe peak patterns when appropriate: s (singlet), d (doublet), t (triplet), q (quadruplet), m (multiplet). Mass spectra of the final products were obtained with a LCQ Thermoquest ion trap mass spectrometer. Where analyses are indicated only by the symbols of the elements, results are within ±0.4% of the theoretical values. All reactions were followed by TLC, carried out on Merck silica gel 60 F_{254} plates with fluorescent indicator, and the plates were visualized with UV light (254 nm). Preparative chromatographic purifications were performed using a Kieselgel 60 silica gel column. Solutions were dried over Na_2SO_4 and concentrated with a Büchi rotary evaporator at low pressure.

***N*-(1-Methyl-4-piperidinyl)-4-anisidine (1).** A solution of *p*-anisidine (30 g, 0.243 mol) and 1-methylpiperidin-4-one (21.3 g, 0.189 mol) in dry methanol (250 mL) was stirred for 6 h at room temperature in the presence of molecular sieves (3 Å, 21 g; 5 Å, 21 g). Then acetic acid (150 mL) was added and the mixture was stirred for 14 h. $NaBH_3CN$ (7.74 g, 0.123 mol) was added, and the resulting solution was stirred for another 3 h. After filtration, the molecular sieves were washed with methanol. The solvent was evaporated, and the crude material was then dissolved in ethyl acetate (350 mL) and washed with brine (3 × 50 mL) and water (50 mL). The organic layer was dried on anhydrous Na_2SO_4 and filtered, and the solvent was evaporated. After chromatography on a silica gel column (eluent, 6:4 dichloromethane/methanol) 28 g of **1** was obtained (68%) as an oil.

***N*-(1-Methyl-4-piperidinyl)-4-anisylhydrazine (2).** Compound **1** (19.5 g, 0.089 mol) in absolute ethanol (240 mL) was cooled to 0 °C and mechanically stirred. Then 37% HCl (190 mL) was added slowly. A solution of $NaNO_2$ (7.93 g, 0.115 mol) in H_2O (50 mL) was added dropwise, keeping the mixture below 0 °C. After completion of the addition, the solution was stirred at this temperature for 3 h. Then water (600 mL) was added, and the mixture was made alkaline with 6 N NaOH. The solution was extracted with ethyl acetate (3 × 200 mL), washed with water, dried on anhydrous Na_2SO_4, and filtered, and the solvent was evaporated. The crude nitroso compound was used without further purification. A suspension of $LiAlH_4$ (9.5 g) in THF (84 mL) was heated to reflux. The crude nitroso compound (25 g) in THF (60 mL) was added dropwise. The mixture was stirred at reflux for 1 h and then cooled to room temperature. Successively, water (15 mL) and aqueous 3 N NaOH (15 mL) were added dropwise. The mixture was filtered on Celite, and the residue was washed several times with dichloromethane. The solvent was removed, obtaining 18.7 g of **2** (90%).

[5-Methoxy-2-methyl-1-(1-methylpiperidin-4-yl)-1*H*-indol-3-yl]acetic Acid Ethyl Ester (3). A solution of the hydrazine derivative **2** (18.7 g, 0.080 mol) and ethyl levulinate (11.52 g, 0.080 mol) in absolute ethanol (430 mL) was stirred and heated to reflux for 18 h. After evaporation of the solvent, ethyl acetate (300 mL) was added. The organic phase was washed with brine, dried on anhydrous $MgSO_4$, and filtered, and the solvent was evaporated. Sulfuric acid (96%, 4 mL) was added to a residue dissolved in absolute ethanol, and the mixture was heated to reflux for 18 h. Then the solution was made alkaline with 1 N NaOH. Ethanol was removed and the extraction performed with ethyl acetate (3 × 150 mL). The organic layers were washed with brine, dried on anhydrous $MgSO_4$, and filtered, and the solvent was evaporated. After chromatography on silica gel column (eluent, 94:0.5:1 dichloromethane/methanol/NH_4OH), a yield of 19.7 g of **3** was obtained (71%): mp 68−70 °C.

[5-Methoxy-2-methyl-1-(1-methyl-piperidin-4-yl)-1*H*-indol-3-yl]acetic Acid (4). To a solution of **3** (8 g, 0.022 mol) in ethanol (140 mL), an amount of 80 mL of 1 N NaOH was added. The mixture was stirred for 2 h at room temperature. Then the solution was neutralized with 1 N HCl. Ethanol was removed and the extraction performed with ethyl acetate (3 × 150 mL). The organic layers were washed with brine, dried on anhydrous $MgSO_4$, and filtered, and the solvent was evaporated, yielding 6.8 g of **4** (98%) as a white solid: mp 172−173 °C.

[5-Hydroxy-2-methyl-1-(1-methylpiperidin-4-yl)-1*H*-indol-3-yl]acetic Acid·HI (5). To a mixture of **4** (3.2 g, 0.010 mol) and acetic anhydride (16 mL) was added 57% hydroiodic acid (7.8 mL). The mixture was stirred for 2 h at 130 °C. Successively, the mixture was cooled to 0 °C, alkalinized with 5% $NaHCO_3$, and then extracted with dichloromethane (3 × 50 mL). The organic layers were washed with brine, dried on anhydrous $MgSO_4$, and filtered, and the solvent was evaporated. The crude compound was recrystallized from diethyl ether, yielding 1.2 g of **5** (40%) as a solid: mp 204−206 °C.

[5-Acetoxy-2-methyl-1-(1-methylpiperidin-4-yl)-1*H*-indol-3-yl]acetic Acid Ethyl Ester (6). To a mixture of **3** (3.2 g, 0.010 mol) and acetic anydride (16 mL) was added 57% hydroiodic acid (7.8 mL). The mixture was stirred for 2 h at room temperature. Successively, the mixture was cooled to 0 °C, alkalinized with 5% $NaHCO_3$, and then extracted with dichloromethane (3 × 50 mL). The organic layers were washed with brine, dried on anhydrous $MgSO_4$, and filtered, and the solvent was evaporated. The crude compound was recrystallized from diethyl ether, yielding 1.1 g of **6** (30%) as a solid: mp 98−99 °C.

Pharmacology. Cell Culture. The murine monocyte/macrophage J774 cell line was grown in Dulbecco's modified Eagle medium (DMEM) supplemented with 2 mM glutamine, 25 mM HEPES, penicillin (100 μg/mL), streptomycin (100 μg/mL), 10% fetal bovine serum (FBS), and 1.2% sodium pyruvate (Bio Whittaker, Europe). Cells were plated in 24-well culture plates at 2.5×10^5 cells/mL or in 10 cm diameter culture dishes ($1 \times l0^7$ cells/l0 mL per dish) and allowed to adhere at 37 °C in 5% CO_2/95% O_2 for 2 h. Immediately before the experiments, the culture medium was replaced by fresh medium without FBS to avoid interference with the radioimmunoassay and cells were stimulated as previously described.[16]

Assessment of COX-1 Activity. Cells were pretreated with reference or test compounds (0.01−100 μM) for 15 min and further incubated at 37 °C for 30 min with 15 μM arachidonic acid to activate the constitutive COX.[8] Stock solutions of reference and test compounds were prepared in ethanol, and equivalent amounts of ethanol were included in the control samples. At the end of the incubation the supernatants were collected for measurement of PGE2 by radioimmunoassay.[17]

Assessment of COX-2 Activity: Exogenous Substrate. J774 cells were stimulated for 24 h with *S. thyphosa* lipopolysaccharide (LPS, 10 μg/mL) to induce COX-2. The supernatant of the cells was replaced with fresh medium containing arachidonic acid (15 μM) in the absence (controls) or presence of test compounds (0.01−100 μM). Then cells were incubated for 30 min at 37 °C and the supernatant was collected for the measurement of PGE2 by radioimmunoassay.[13] Stock solutions of reference and test compounds were prepared in ethanol, and equivalent amounts of ethanol were included in the control samples.

Chemical Stability of 3. Blood was withdrawn by cardiac puncture from mice (18−20 g) and plasma obtained by centrifugation (12 000 rpm, 4 °C). Citrate (3.8%v/w) was used as anticoagulant. Liver was obtained from mice and homogenized in RIPA buffer (1 mg/1 mL). **3** (1 mg/mL) was dissolved in DMSO and left to incubate with plasma or liver homogenate. The compounds were incubated at 37 °C, and samples for analysis were taken after

30 or 60 min of incubation. Levels of **4** were monitored by HPLC analysis. Reversed-phase analysis was routinely performed on a Waters 600 system using a Vydac C18 silica (5 μm, 4.6 mm × 250 mm) HPLC column. The elution was performed with the following conditions: eluent A, 0.05% TFA (v/v) in water; eluent B, 0.05% TFA (v/v) in acetonitrile; gradient 10−80% B over 25 min; UV detection at 254 nm; flow rate of 1 mL/min. The HPLC analysis gave the following results: **3** at t_R = 14.34 min and **4** at t_R = 10.25 min.

Mouse Paw Edema. Mice (18−20 g) were separated in groups and lightly anesthetized with enflurane. Each group received subplantar injection of 50 μL of carrageenan, 1 wt %/vol, into the left footpad. Paw volume was measured by using a hydroplethismometer modified for small volume (Ugo Basile, Italy) immediately before the subplantar injection and 2, 4, 6, 24, 48, and 72 h thereafter. The increase in paw volume was evaluated as the difference between the paw volume at each time point and the basal paw volume. Mice were treated 1 h prior to the injection of carrageenan with **3**−**6**.

Acetic Acid Induced Writhing. Male Swiss mice (25−30 g) were injected intraperitoneally with acetic acid (0.6%) in a final volume of 500 μL. The mice were placed in individual cages for observation. After the first writhing movement appeared, the animals were kept under observation for 15 min and the number of writhings was counted during this period.

Formalin Paw Licking. Mice (18−20 g) were treated 1 h prior to the injection of formalin with gabapentin or **3**−**6**. Injection of 10 μL of formalin (5%) in the plantar area was performed under light anesthesia with enflurane. Mouse paw licking behavior was evaluated for two periods by an observer unaware of the treatment: first phase, 0−15 min; second phase, 15−45 min.

Acute Gastric Damage. Rats (120−140 g) were deprived of food but not water for 18 h and were then given **3**−**6** orally at a dose of 100 mg/kg. Another group was treated with an equal volume of the vehicle. Each group consisted of six rats. After 5 h, the rats were anesthetized with sodium pentobarbital and the stomach was excised and opened by an incision along the greater curvature. The extent of macroscopic damage was determined by an observer unaware of the treatments that the rats had received, as previously described.[18] The method involved measuring the lengths of the lesions in millimeters and then adding the lengths of all lesions observed in each stomach. Data were analyzed by ANOVA for the nonparametric Kruskall−Wallis test followed by Dunn's post-test.

Statistical Analysis of Pharmacological Data. Triplicate wells were used for the various treatment conditions. Results are expressed as the mean of three experiments for the percent of inhibition of PGE2 production by reference and test compounds with respect to control samples. Data (nanograms of PGE2 produced) were analyzed by using one-way ANOVA followed by a Bonferroni post hoc test for multiple comparisons. A p value less than 0.05 was considered statistically significant.

Molecular Modeling. All calculations were performed with the DISCOVER program (Accelrys, San Diego, CA) on Silicon Graphics O2 R5000 computers (SGI, Mountain View, CA). The force field CVFF with a time step of 1 fs and a cutoff of 12 Å for the nonbonded interactions was employed for all calculations. A distance-dependent dielectric constant $\epsilon = 4r$ (r in Å) was used for mimicking the dielectric properties inside the protein molecule. The published X-ray structure of the COX-2 enzyme in complex with indomethacin[11] (PDB code 4COX) was used as the starting point for the molecular modeling. Indomethacin and our new compounds **3**−**6** are almost completely buried within the receptor, and we have therefore not included explicitly the solvent to speed up the calculations. A generous binding site around indomethacin was allowed to move freely during the MD simulations, and no artificial constraints were imposed on the ligands. To enhance the stability of the protein structure during the simulation, especially at higher temperatures, all parts of the enzyme that are far from the binding site were fixed in space. Amino acid residues of the COX-2 protein that had in the X-ray structure at least one atom closer than 7 Å to indomethacin (meaning any atom of indomethacin) were allowed to move without artificial constraints to allow for an induced fit. Thus, a flexible binding site for COX-2 consisting of Val-89, His-90, Leu-93, Thr-94, Met-113, Val-116, Leu-117, Ser-119, Arg-120, Gln-192, Phe-198, Phe-205, Thr-206, Val-344, Ile-345, Tyr-348 to Tyr-355, Phe-357, Leu-359, Phe-381, Leu-384, Tyr-385, Trp-387, Val-434, Leu-507, Arg-513, Ala-516 to Lys-532, and Leu-534 was constructed. **3**−**6** were placed inside the enzyme by superimposition on heavy atoms that are common to indomethacin and the new inhibitor molecules. For this purpose the piperdine of **3**−**6** was oriented in the same way as the phenyl ring of indomethacin. The protonation states were positively charged for the piperadine moiety and negatively charged for the 3-acetic acid substituent occurring only in **4** and **5**. For the generation of the COX-1/indomethacin complex models, two crystallographically determined complex structures comprising COX-1 (PDB code 1DIY) and COX-2 (PDB code 1CVU) in complex with the same ligand (i.e., arachidonic acid) were compared. Both structures were found to be very similar in the general fold and in the specific details of the binding site, although crystallographic *B* factors that are a measure of local flexibility or heterogeneity are generally larger for the COX-1 than for the COX-2 complex. Several other COX/inhibitor complex structures ((COX-1) 1EBV, 1PGG; (COX-2) 1PTH, 1CX2, 6COX) also exhibited similarities. Therefore, the coordinates of COX-1 of the 1DIY structure were superimposed on those of COX-2 of the COX-2/**3**−**6** starting structure, thus generating the COX-1/**3**−**6** starting model. The COX-1/indomethacin complex was built in the same way as all calculations were carried out for **3**−**6** and indomethacin as ligands, with indomethacin serving as a reference. The flexible binding site of COX-1 comprised the same part of the sequence as for COX-2 but with a few changes in amino acid residue types due to the differences in sequence between the two COX isoforms. The following changes occur within the 7 Å binding area when moving from COX-1 to COX-2: I89V, V119S, Q351H, L357F, I434V, H513R, S516A, S521T, I523V, M525L. In the first step of the calculations the model complex consisting of the COX-1 or COX-2 enzyme and the respective ligand was energy-minimized to relax steric clashes generated by the placement of the inhibitor. MD simulated annealing of the complex was started at 10 K (for 10 ps). Coupling to a temperature bath (time constant of 1 ps) with stepwise increasing target temperatures served to heat the simulation system gradually. After 50 ps at 100 K the most relevant part of 100 ps at 300 K was followed by an additional 50 ps at 500 K to test for the stability of the complex established at 300 K.

Acknowledgment. The NMR spectral data were provided by Centro di Ricerca Interdipartimentale di Analisi Strumentale, Università degli Studi di Napoli "Federico II". The assistance of the staff is gratefully appreciated.

Supporting Information Available: NMR, MS, and elemental analysis data. This material is available free of charge via the Internet at http://pubs.acs.org.

References

(1) Roller, A.; Bahr, O. R.; Streffer, J.; Winter, S.; Heneka, M.; Deininger, M.; Meyermann, R.; Naumann, U.; Gulbins, E; Weller, M. Selective potentiation of drug cytotoxicity by NSAID in human glioma cells: the role of COX-1 and MRP. *Biochem. Biophys. Res. Commun.* **1999**, *259*, 600−605.

(2) Lu, J. X.; Shen, Qi.; Jiang, J. H.; Shen, G. L.; Yu, R. Q. QSAR analysis of cyclooxygenase inhibitor using particle swarm optimization and multiple linear regression. *J. Pharm. Biomed. Anal.* **2004**, *35*, 679−687.

(3) Selvam, C.; Jachak, S. M.; Thilagavathi, R.; Chakraborti, A. K. Design, synthesis, biological evaluation and molecular docking of curcumin analogues as antioxidant, cyclooxygenase inhibitory and anti-inflammatory agents. *Bioorg. Med. Chem. Lett.* **2005**, *15*, 1793−1797.

(4) Chen, Q. H.; Rao, P. N. P.; Knaus, E. E. Design, synthesis, and biological evaluation of *N*-acetyl-2-carboxybenzenesulfonamides: a novel class of cyclooxygenase-2 (COX-2) inhibitors. *Bioorg. Med. Chem.* **2005**, *13*, 2459−2468.

(5) Rao, P. N. P.; Uddin, Md. J.; Knaus, E. E. Design, synthesis, and structure−activity relationship studies of 3,4,6-triphenylpyran-2-ones as selective cyclooxygenase-2 inhibitors. *J. Med. Chem.* **2004**, *47*, 3972−3990.
(6) Grosser, T.; Fries, S.; FitzGerald, A. G. Biological basis for the cardiovascular consequences of COX 2 inhibition: therapeutic challenges and opportunities. *J. Clin. Invest.* **2006**, *116*, 4−15.
(7) Cullen, L.; Kelly, L.; Connor, S. O.; Fitzgerald, D. J. Selective cyclooxygenase-2 inhibition by nimesulide in man. *J. Pharmacol. Exp. Ther*. **1998**, *287* (2), 578−582.
(8) Futaki, N.; Takahashi, S.; Kitagawa, T.; Yamakawa, Y.; Tanaka, M.; Higuchi, S. Selective inhibition of cyclooxygenase-2 by NS-398 in endotoxin shock rats in vivo. *Inflammation Res.* **1997**, *46* (12), 496−502.
(9) Kirchner, T.; Argentieri, D. C.; Barbone, A. G.; Singer, M.; Steber, M.; Ansell, J.; Beers, S. A.; Wachter, M. P.; Wu, W.; Malloy, E.; Stewart, A.; Ritchie, D. M. Evaluation of the anti-inflammatory activity of a dual cyclooxygenase 2 selective/5-lipoxygenase inhibitor, RWJ 63556, in a canine model of inflammation. *J. Pharmacol. Exp. Ther*. **1997**, *282* (2), 1094−1101.
(10) Borch, R. F.; Berstein, M. D.; Durst, H. D. Cyanohydridoborate, anion as a selective reducing agent. *J. Am. Chem. Soc.* **1971**, *93*, 2897−2904.
(11) Westheimer, F. H.; Taguchi, K. Catalysis by molecular sieves in the preparation of ketimines and enamines. *J. Org. Chem.* **1971**, *36*, 1570−1572.
(12) Wallace, J. L.; Mcnight, W.; Reuter, B. K. NSAID-induced gastric damage in rats: requirement for inhibition of both cyclooxygenase 1 and 2. *Gastroenterology* **2000**, *119* (3), 706−714.
(13) Brenneis, C.; Maier, T. J.; Schmidt, R.; Hofacker, A.; Zulauf, L.; Jakobsson, P. J.; Scholich, K.; Geisslinger, G. Inhibition of prostaglandin E2 synthesis by SC-560 is independent of cyclooxygenase 1 inhibition. *FASEB J.* **2006**, *20*, 1352−1360.
(14) Martinez, R. V.; Reval, M.; Campos, M. D.; Terron, J. A.; Dominguez, R.; Lopez-Munoz, F. J. Involvement of peripheral cyclooxygenase-1 and cyclooxygenase-2 in inflammatory pain. *J. Pharm. Pharmacol.* **2002**, *54*, 405−412.
(15) Kurumbail, R. G.; Stevens, A. M.; Gierse, J. K.; Mcdonald, J. J.; Stegeman, R. A.; Pak, J. Y.; Gildehaus, D.; Miyashiro, J. M.; Penning, T. D.; Seibert, K.; Isakson, P. C.; Stallings, W. C. Structural basis for selective inhibition of cyclooxygenase-2 by anti-inflammatory agents. *Nature* **1996**, *384*, 644−648.
(16) Zingarelli, B.; Southan, G. J.; Gilad, E.; O'Connor, M.; Salzman, A. L.; Szabò, C. The inhibitory effects of mercaptoalkylguanidines on cyclooxygenase activity. *Br. J. Pharmacol.* **1997**, *120*, 357−366.
(17) Sautebin, L.; Lanaro, A.; Rombolà, L.; Ialenti, A.; Sala, A.; Di Rosa, M. Cyclooxygenase-2-dependent generation of 8-epiprostaglandin $p2_a$ by lipopolysaccharide-activated J774 macrophages. *Inflammation Res.* **1999**, *48*, 503−508.
(18) Davies, N. M.; Roseth, A. G.; Aplleyard, C. B.; McKnight, W.; Del Soldato, P.; Calignano, A.; Cirino, G.; Wallace, J. L. NO-naproxen vs. naproxen: ulcerogenic, analgesic and anti-inflammatory effects. *Aliment. Pharmacol. Ther.* **1997**, *11*, 69−79.

JM0608199